American Mineralogist, Volume 72, pages 605–609, 1987

Oxygen in pyrrhotite: 2. Determination of oxygen in natural pyrrhotites

JAMES GRAHAM
Division of Minerals and Geochemistry, CSIRO, Wembley, Western Australia 6014, Australia
C. D. MCKENZIE
Physics Department, University of Melbourne, Parkville, Victoria 3052, Australia

ABSTRACT

The nuclear microprobe, using an O(d,p) reaction, can measure the bulk oxygen content independently of surface contamination, and it is shown that in the examples studied the base oxygen level in both hexagonal and monoclinic pyrrhotites at room temperature is about 0.05% oxygen. However, the monoclinic pyrrhotite shows large fluctuations of oxygen content on a micrometer scale, indicating the presence of oxide inclusions.

INTRODUCTION

Evidence for the presence of oxygen in solid solution in pyrrhotite has so far been somewhat indirect [see, for example, the preceding paper in this issue by Graham et al. (1987)]. To confirm the levels of oxygen inferred from the magnetic results, a suitable direct method of analysis was required.

A first attempt to measure solid-solution oxygen in natural pyrrhotites made use of neutron-activation analysis (analyst A. Volborth). Samples were finely ground under petroleum ether and carefully separated by a.c. magnet and by heavy liquids, but there was still contamination from surface-adsorbed oxygen and from micro-inclusions of oxides and silicates. Nevertheless, results were encouraging, as two monoclinic pyrrhotites gave 1.6% (Mt. Morgan) and 0.62% oxygen (Renison Bell), whereas a sample of the hexagonal variety (Nairne) assayed 0.35%.

When discs of natural monoclinic pyrrhotite were being thinned for transmission-electron microscopy, it was almost invariably found that the erosion rate was not uniform across the area of the sample and that a fine network of oxides or silicates was left when the thickness was reduced almost to zero. It therefore appeared necessary to use a micro-analytical method with a resolution of only a few micrometers.

The few methods available for low-level micro-analysis of oxygen in pyrrhotites all require highly specialized equipment. The nuclear microprobe (Cookson et al., 1979) is among the most versatile, as it can make use of Rutherford scattering and nuclear reaction techniques, and also makes possible monitoring for matrix variation and impurities using proton-induced X-ray emission (PIXE). For the detection of light elements such as oxygen in a heavier matrix, nuclear reaction techniques are favored. These techniques make use of reactions between the incident particles and the oxygen in the sample to produce secondary particles that can be positively identified.

The Harwell microprobe (Cookson, 1979) was used for this investigation; it is capable of adequate ion currents for nuclear reaction techniques even when finely focused. Two different pyrrhotites were examined: a hexagonal variety from Nairne in South Australia, which was available in large "single-phase" areas (grain-boundary impurities such as monoclinic pyrrhotite and other transition-metal sulfides could generally be avoided), and a monoclinic pyrrhotite from Kambalda, Western Australia, containing some inclusions of pentlandite, magnetite, and pyrite.

Our nuclear reaction technique made use of thick specimens (>100 μm) with the deuteron beam incident normally, and the proton spectrum detected at a deflection angle of 135° from the incident beam using a Si surface-barrier detector and multichannel analyzer. Polished specimens were prepared by normal metallographic techniques, using diamond paste on a Pb lap with hydrocarbon lubricant for the final polish. They were then ultrasonically cleaned in a solvent, hand-lapped with 0.3-μm alumina for a few seconds, washed with water and absolute alcohol, then lightly rubbed with a tissue (specimen A). Any residues of light elements on the surface are to be avoided, since they introduce unwanted background.

Further specimens were prepared by etching the above (to minimize surface oxidation) by electrolysis at a cathode potential of −0.2 V relative to a saturated calomel

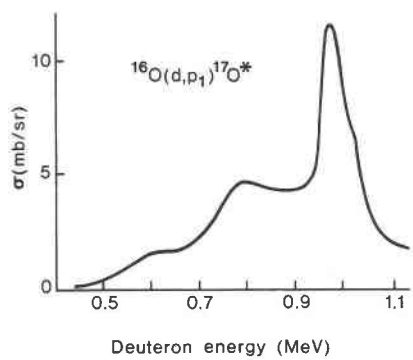

Fig. 1. Cross section for the reaction $^{16}O(d,p_1)^{17}O^*$.

0003–004X/87/0506–0605$02.00

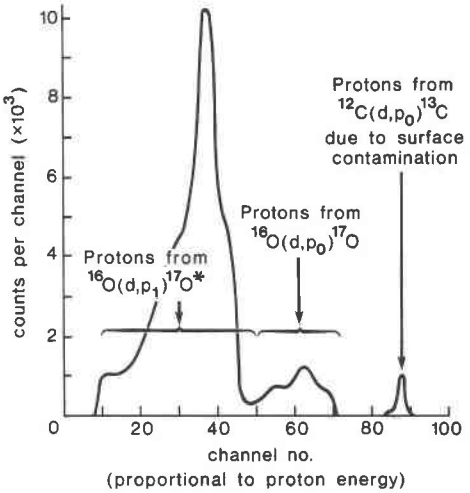

Fig. 2. Energy spectrum of emitted protons from a crystal of pure magnetite bombarded with deuterons of energy 1.10 MeV.

electrode in a solution of 0.3*M* NaCl and 0.1*M* HCl for 10 min. They were washed in H_2-saturated water and dried with a tissue in air (specimen B). This etching was visible microscopically and, where the orientation was unfavorable, gave a rough surface that possibly allowed access for oxygen. Grains with the close-packed planes parallel to the surface should have been more resistant to oxidation.

A third set of specimens was prepared by etching the polished material in 1*M* HCl with H_2 bubbling through for 1 h. They were washed with H_2-saturated distilled water and dried with a tissue under a stream of H_2 (specimen C). The surface should probably consist of a mosaic of anodically and cathodically etched areas (respectively more and less oxidized), but the only visible effect of the etch was to make the inclusions slightly sharper in outline.

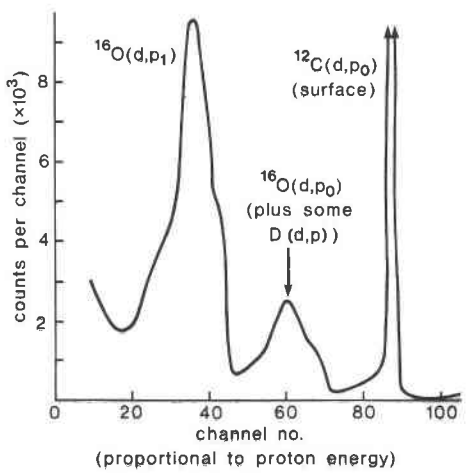

Fig. 3. The proton spectrum from monoclinic pyrrhotite KA.

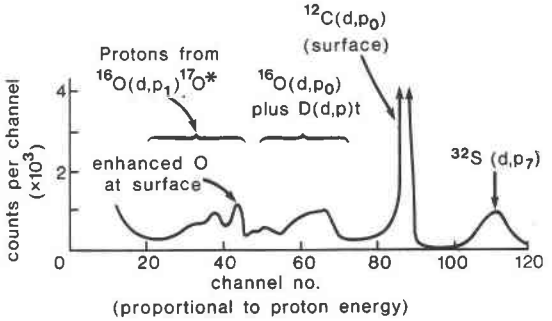

Fig. 4. The proton spectrum from hexagonal pyrrhotite NA. The peak at channel 44 is due to enhanced surface oxygen. The $^{32}S(d,p_7)^{33}S$ peak at channel 110 is a guide to another S interference at channel 33, which becomes significant at low oxygen contents.

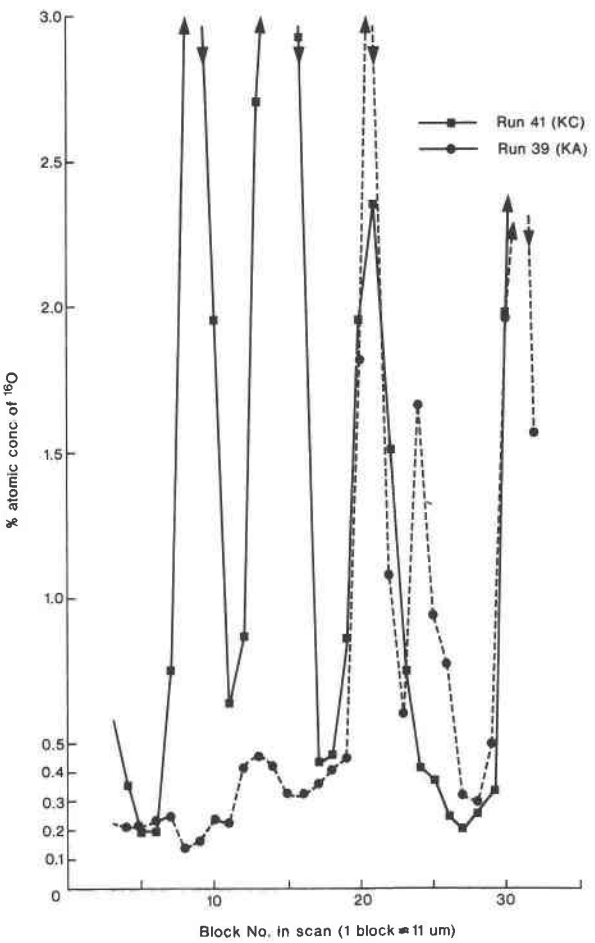

Fig. 5. Bulk oxygen distribution in pyrrhotite (linear scans). Atomic percent ^{16}O just below the surface is plotted against step number (distance along the scan). Beam size is 15 × 15 μm, and step length is about 11 μm. Total length of scan is 360 μm. In the sample designation, the first letter refers to Kambalda and Nairne (monoclinic and hexagonal, respectively) and the second letter to the method of preparation (see text).

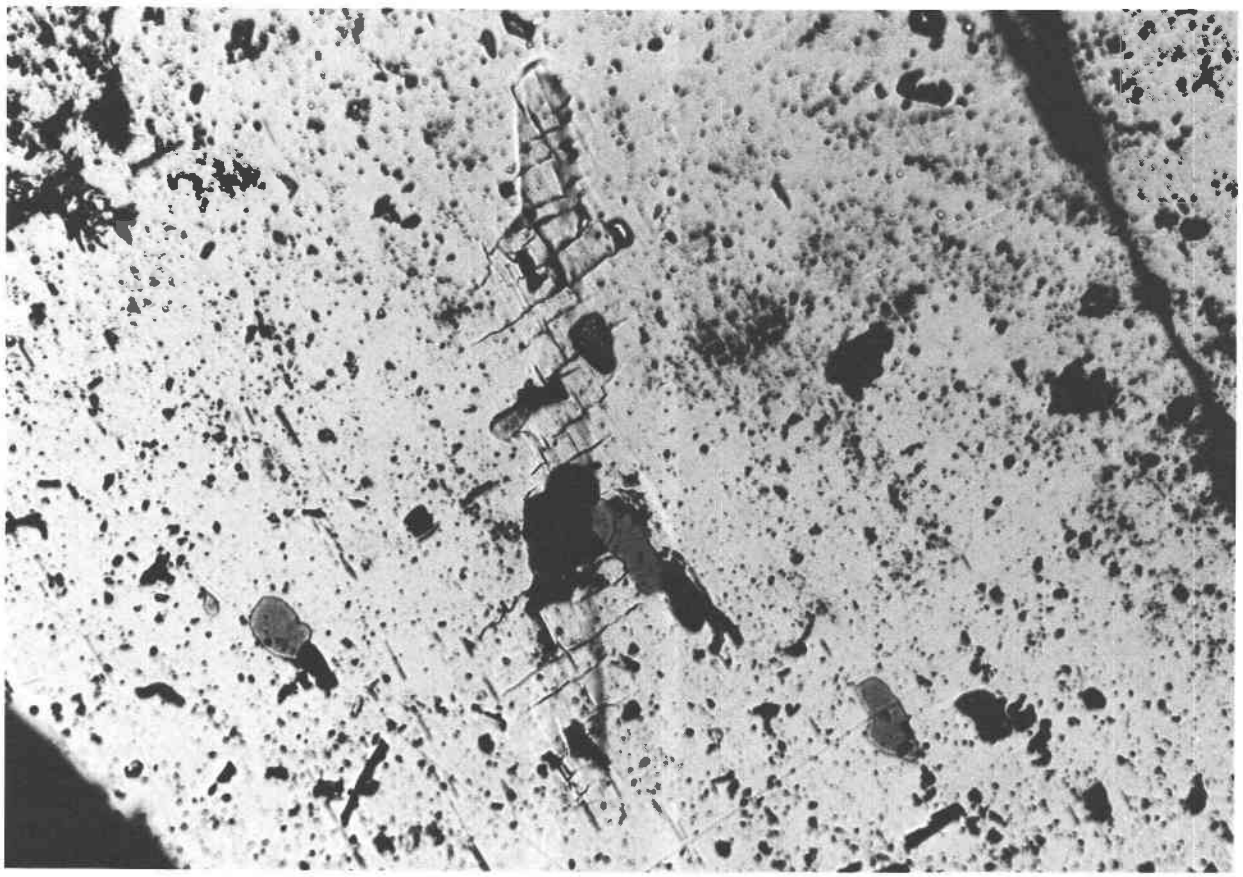

Fig. 6. Micrograph of scan on sample KA. Dirty surface some months after run. Light gray = pyrrhotite, medium gray = magnetite, black = cracks and spalled areas. Oxygen peaks correspond to cracks and magnetite inclusions. Length of scan, 360 μm.

The nuclear reaction method

For maximum sensitivity and freedom from contaminant reactions, most of our work was carried out using the nuclear reaction $^{16}O(d,p_1)^{17}O^*$ at an incident deuteron energy of 1.10 MeV. (The nomenclature means that the protons p_1 produced by reaction with the incident deuterons, d, have an energy such that the ^{17}O nucleus is left in its first excited state.) The excitation function for this reaction at an observation angle of 135° (i.e., the probability of the reaction as a function of deuteron energy) is shown in Figure 1—see, for example, Kim et al. (1964) and Mayer and Rimini (1977). The deuterons will lose energy as they penetrate the sample, so that a beam of 1.1-MeV deuterons will have maximum sensitivity for the reaction at 1.7 μm below the surface and will minimize the response to surface-adsorbed oxygen. Because the emergent protons also lose energy as a function of their path length in the solid, protons with a given energy loss will correspond to a nuclear reaction at a given depth. It is therefore possible, using the cross section of Figure 1, to measure the oxygen content as a function of depth; and if oxygen is uniformly distributed through the target, the energy distribution of the emerging protons will closely resemble the excitation function.

This is illustrated in Figure 2, which is the proton spectrum from a single crystal of pure magnetite. This spectrum was used to calibrate the oxygen sensitivity. The sharp peak at channel 87 is due to protons from the reaction $^{12}C(d,p_0)^{13}C$, generated in a thin surface-contamination layer.

Oxygen levels are, of course, orders of magnitude lower in the pyrrhotite samples, but the same trends can be seen. Figure 3 shows the spectrum from a large area (15 × 360 μm^2) of a Kambalda monoclnic pyrrhotite, which indicates an approximately uniform depth distribution of oxygen. This spectrum results from all data leading to Figure 5; the sample in question (KA) contained small regions rather rich in oxygen and is dicussed in more detail shortly. Figure 4, a spectrum of Nairne pyrrhotite, is typical in showing low levels of total oxygen and allowing one to see a peak at higher energy (channel 44) indicating the presence of surface-adsorbed oxygen. A calibration run with a specimen of metallic Al showed only this peak. At low oxygen concentration, the small peak due to the D(d,p)t reaction (from deuterium beam par-

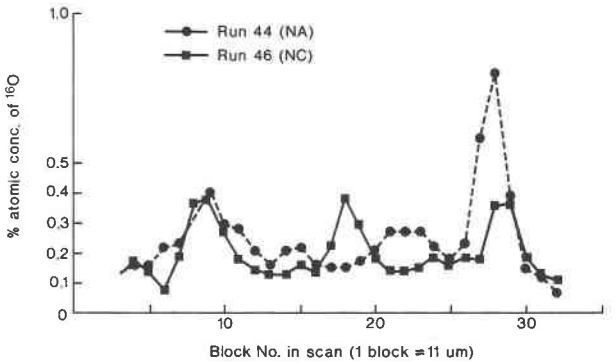

Fig. 7. Oxygen in hexagonal pyrrhotite. See caption to Figure 5. Even hexagonal pyrrhotite shows some irregular enrichment of oxygen.

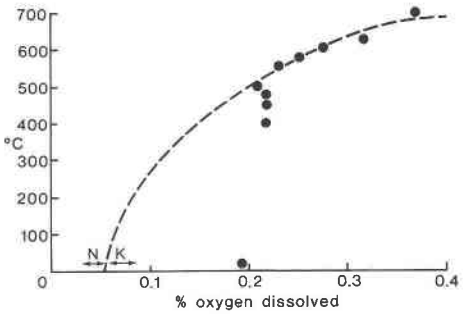

Fig. 8. Solubility of oxygen as a function of temperature in monoclinic pyrrhotite. Filled circles are magnetic results from Table 1. Arrows show range by nuclear reaction measurements for Kambalda (K) and Nairne (N) samples.

ticles stopped and trapped in the sample) becomes more important, overlapping the $^{16}O(d,p_0)^{17}O$ output. Figure 4 also shows some higher energy protons from $^{32}S(d,p_7)$.

These interferences are deduced from observation of calibration standards and from the results of Caplain et al. (1982). The only significant interference from S is from the $^{32}S(d,p_{32})^{33}S$ reaction, where p_{32} indicates that the outgoing proton has left the ^{33}S in its 32nd excited state. These protons should give a peak at channel 33, and its intensity can be monitored by that of the $^{32}S(d,p_7)$ peak already referred to. We have chosen to represent volume ^{16}O by the sum of counts in channels 35–40, thus avoiding the surface oxygen and the interferences.

Some orientation runs were carried out with a stationary beam typically about 45 × 30 μm in size. This beam size is too large to avoid the inhomogeneities subsequently found in the scanned runs, but indicated, as the bulk techniques had done, that the monoclinic pyrrhotite from Kambalda contained a higher overall oxygen concentration than the Nairne hexagonal pyrrhotite. Similarly, some results on the electrolytically etched sample showed that areas with the **c** axis inclined to the surface did adsorb oxygen along the basal planes—the average of two readings on "dark" areas was 0.3% compared with 0.06% O in a "light" area with the **c** axis perpendicular to the surface.

The definitive runs (Figs. 5–7) were carried out with a beam size of 15 × 15 μm, continuously scanned by electrostatic deflection over a distance of 360 μm. Events were sorted, according to position along the scan line, into 32 blocks (approximately 11 μm per block). The results normally show a fairly low background oxygen level with peaks occurring at various points along the scan; the peaks are correlated with pits and small magnetite grains.

Between the peaks, the background levels are in the range 0.03–0.05% (0.09–0.13 atomic percent) oxygen for the Nairne samples and 0.05–0.08% (0.13–0.22 atomic percent) oxygen for Kambalda. In the case of Nairne, no magnetite has been observed magnetically, but the magnetic balance method involves heating, which tends to dissolve any magnetite so that the presence of traces of magnetite at room temperature cannot be ruled out. The peaks in the oxygen scan may therefore correspond to small amounts of magnetite, and the value of 0.05% oxygen may correspond to saturation at room temperature. There is a wide range of background values for Kambalda material, and this may reflect the greater inhomogeneity of the samples. The lowest value roughly corresponds to the oxygen content of Nairne, reinforcing the idea that the saturation value is at least as low as this. However, saturation may occur at different oxygen contents at different metal/S ratios, and the average value from Kambalda of about 0.07% may represent the saturation value for Fe_7S_8.

Saturation values of about 0.07% oxygen are consistent with the data of Table 1 of Graham et al. (1987), as shown in Figure 8. The data at high temperatures are for sample STD3, and diffusion has evidently ceased at temperatures a little below 500°C. Using a slow-cooling technique and another sample, it has been possible to precipitate magnetite more freely at lower temperatures. Between room temperature and 600°C, an additional 0.8% magnetite (0.2% oxygen) dissolves.

Although this work was intended to be of an exploratory nature, the nuclear reaction technique has already shown that there is a distribution of oxygen throughout the volume of both hexagonal and monoclinic pyrrhotite. Some is undoubtedly in the form of fine magnetite inclusions, giving rise to the observed inhomogeneity in the scans, but at least 0.05% appears to be in solid solution at room temperature. A thin layer of adsorbed oxygen often occurs at the surface, and on an etched surface the oxygen can penetrate rather deeply along the close-packed planes at room temperature.

Summary

It would of course be necessary to perform similar experiments with many samples in order to generalize confidently, and it is proposed to follow up this work on the new CSIRO ion probe at North Ryde, perhaps using a tuned Rutherford backscatter technique. But these experiments have confirmed the presence of solid-solution oxygen in pyrrhotites, and the presence of oxygen-rich

phases in monoclinic pyrrhotite. The layer of adsorbed oxygen on the pyrrhotite surface, which has long been suspected, has also been demonstrated. The surface contamination does not interfere with measurements of oxygen in bulk pyrrhotite.

Acknowledgment

One of us (C. D. McKenzie) must thank the staff of the Nuclear Physics Division, AERE, Harwell, for their kind co-operation and assistance in making the microprobe available for this work.

References

Caplain, R., David, D., and Beranger, G. (1982) La microanalyse du soufre par l'observation des réactions nucléaires. Revue de Physique Appliquée, 17, 441–445.

Cookson, J.A. (1979) The production and use of a nuclear microprobe of ions at MeV energies. Nuclear Instruments and Methods, 165, 477–508.

Cookson, J.A., McMillan, J.W., and Pierce, T.B. (1979) The nuclear microprobe as an analytical tool. Journal of Radioanalytical Chemistry, 48, 337–357.

Graham, J., Bennett, C.E.G., and van Riessen, A. (1987) Oxygen in pyrrhotite: Part 1. Thermomagnetic behavior and annealing of pyrrhotites containing small quantities of oxygen. American Mineralogist, 72, 599–604.

Kim, H.C., Seiler, R.F., Herring, D.F., and Jones, K.W. (1964) Cross sections for the $O^{16}(d,p_0)O^{17}$,$O^{16}(d,p_1)O^{17*}$ and $O^{16}(d,\alpha O)N^{14}$ reactions from 0.8 to 1.7 NeV. Nuclear Physics, 57, 526–530.

Mayer, J.W., and Rimini, E. (1977) Ion beam handbook for material analysis. Academic Press, New York.

Manuscript received March 29, 1985
Manuscript accepted January 26, 1987